

## Supporting Information

### **A Smart 3D Microfluidic Tumor Spheroid-Vessel Co-Culture Model for Studying Exosomal HSP-Mediated Tumor Invasion and Angiogenesis**

Sisi Zhou, <sup>†a</sup> Fanshu Shan, <sup>†b</sup> Yue Zhang, <sup>b</sup> Yu Cao, <sup>b</sup> Junhui Cen, <sup>c</sup> Noritada Kaji <sup>de</sup> and Songqin Liu <sup>\*ab</sup>

<sup>a</sup> Analysis and Testing Center, Southeast University, Nanjing 211189, China

<sup>b</sup> Jiangsu Engineering Laboratory of Smart Carbon-Rich Materials and Device, School of Chemistry and Chemical Engineering, Southeast University, Nanjing 211189, China

<sup>c</sup> School of Materials Science and Engineering, Southeast University, Nanjing 211189, China

<sup>d</sup> Department of Applied Chemistry, Graduate School of Engineering, Kyushu University, 744 Motoooka, Nishi-ku, Fukuoka 819-0395, Japan

<sup>e</sup> Institute of Nano-Life-Systems, Institutes of Innovation for Future Society, Nagoya University, Furo-cho, Chikusa-ku, Nagoya 464-8603, Japan

<sup>†</sup> These authors contributed equally to this work.

\*Corresponding author: E-mail: liusq@seu.edu.cn.

## **Table of Content**

- Fig. S1 Chip design schematics**
- Fig. S2 Schematic diagram of the on-chip cell loading process**
- Fig. S3 Photograph of the medium loaded in the microfluidic chip**
- Fig. S4 Optimization of the width of channels that physically connect the tumor spheroid and endothelial compartments**
- Fig. S5 Spatial position of tumor spheroids within different microwells**
- Fig. S6 On-chip cell density optimization**
- Fig. S7 Tumor spheres grown on the chip for different periods of time**
- Fig. S8 Viability assessment of on-chip tumor spheroids**
- Fig. S9 Viability assessment of on-chip HUVEC cells**
- Fig. S10 Effects of MDA-MB-231-derived exosomes on tumor invasion and angiogenesis under different incubation times**
- Fig. S11 Construction of Exosome<sup>HSP del</sup>**
- Fig. S12 The variation trend of Absorbance versus HSP concentration.**
- Fig. S13 Effects of HSPs concentration on tumor invasion and angiogenesis**

**Fig. S1** Chip design schematics

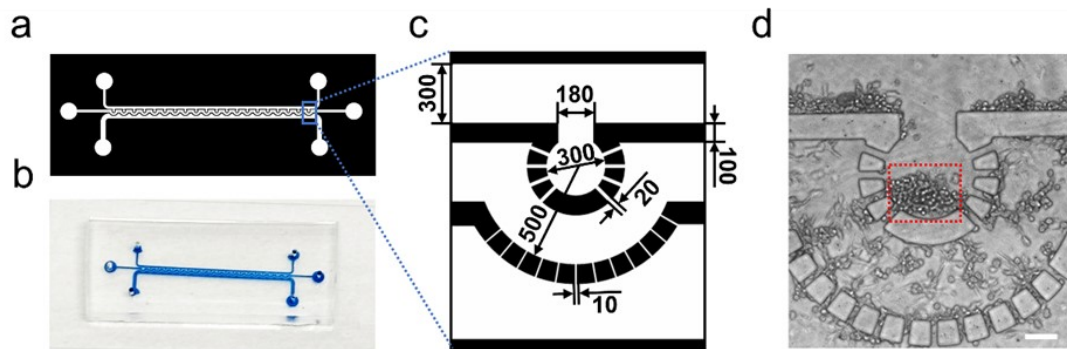


**Fig. S1** Chip design schematics. (a) Photomask design of the chip: black regions are opaque while white areas are transparent. (b) Photograph of the fabricated chip. (c) Magnified view of the photomask: opaque black regions and transparent white regions are shown with dimensional units in  $\mu\text{m}$ . (d) Micrograph of the chip after cell loading: tumor spheroids are contained within the red square, scale bar: 100  $\mu\text{m}$ .

**Fig. S2 Schematic diagram of the on-chip cell loading process**

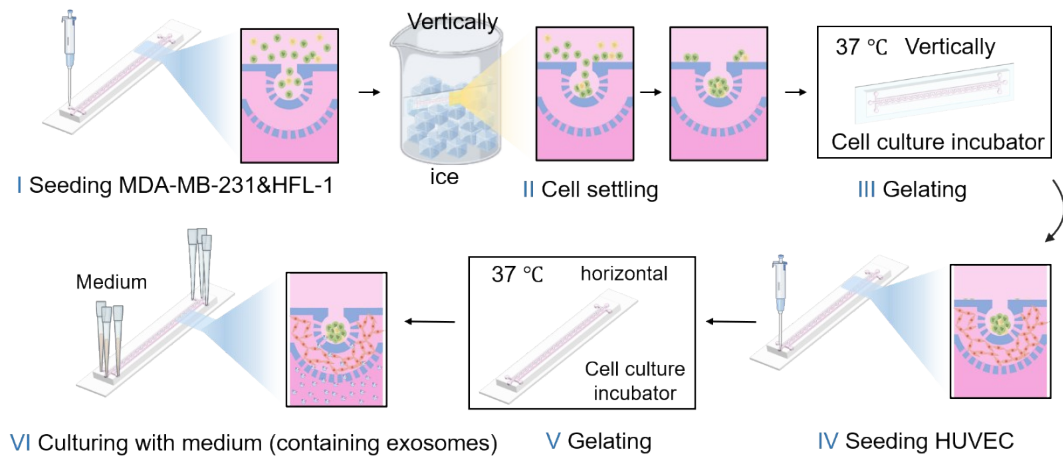


**Fig. S2 Schematic diagram of the on-chip cell loading process.**

**Fig. S3 Photograph of the medium loaded in the microfluidic chip**

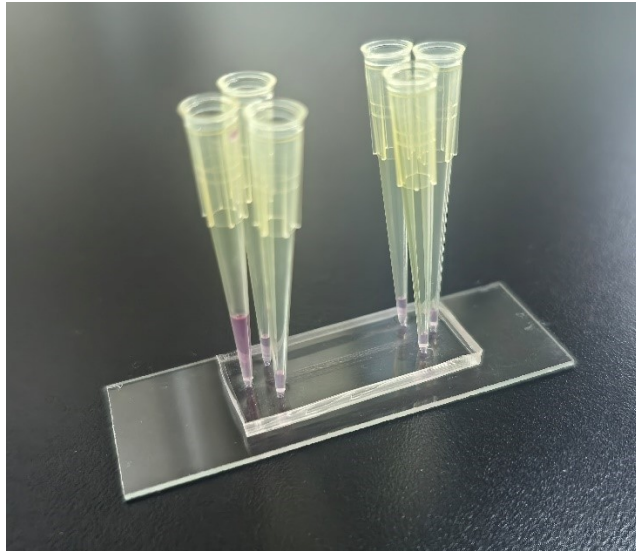


**Fig. S3 Photograph of the medium loaded in the microfluidic chip.**

**Fig. S4 Optimization of the width of channels that physically connect the tumor spheroid and endothelial compartments**

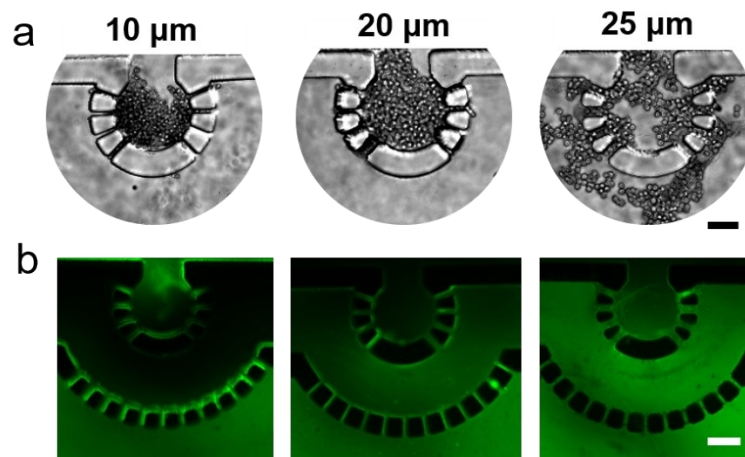


**Fig. S4** Optimization of the width of channels that physically connect the tumor spheroid and endothelial compartments. (a) The distribution of cells within channels of different width (scale bar: 100  $\mu\text{m}$ ). (b) The situation of molecular diffusion 20 minutes after being introduced into channels (scale bar: 150  $\mu\text{m}$ ).

**Fig. S5 Spatial position of tumor spheroids within different microwells**

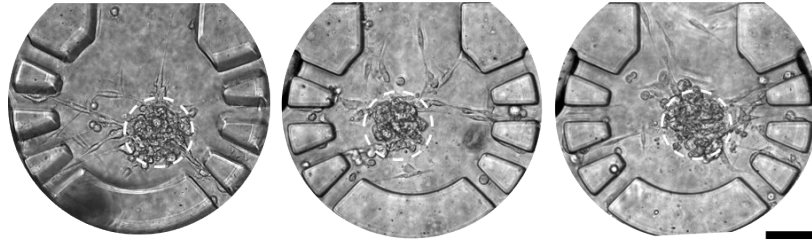


**Fig. S5** Spatial position of tumor spheroids within different microwells (scale bar: 100  $\mu\text{m}$ ).

**Fig. S6 On-chip cell density optimization**

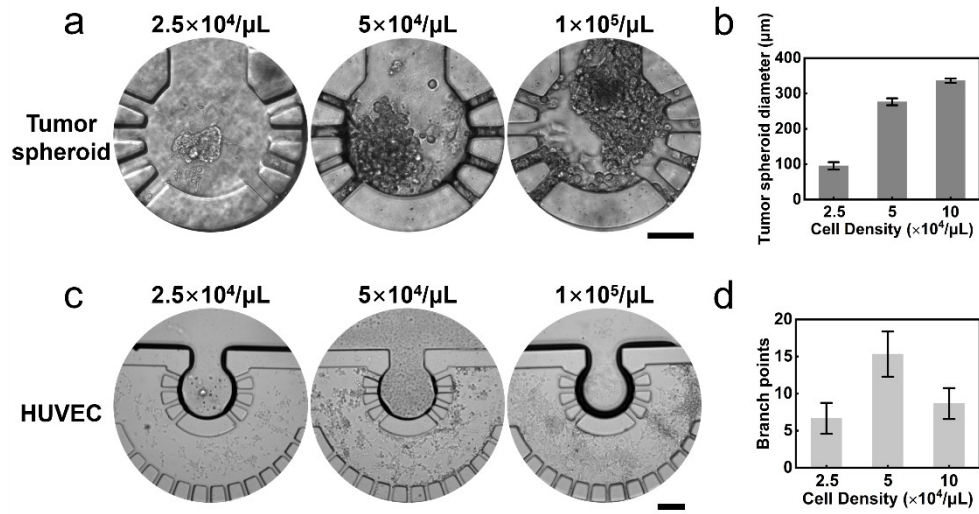


**Fig. S6** On-chip cell density optimization. For tumor spheroids: (a) Bright-field image (scale bar:  $100 \mu\text{m}$ ). (b) Histogram of spheroid diameters under different cell densities (error bars represent triplicate experiments). For HUVECs: (c) Bright-field image (scale bar:  $150 \mu\text{m}$ ). (d) ImageJ-quantified branch points of microvascular networks across densities. Error bars represent triplicate experiments.

**Fig. S7 Tumor spheres grown on the chip for different periods of time**

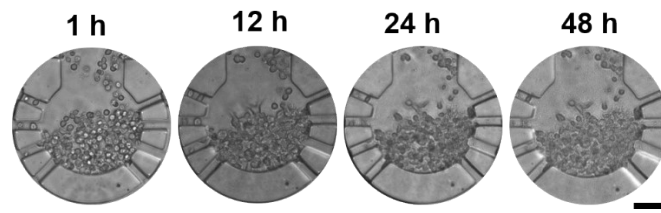


**Fig. S7** Tumor spheres grown on the chip for different periods of time (scale bar: 100  $\mu\text{m}$ ).

**Fig. S8 Viability assessment of on-chip tumor spheroids**

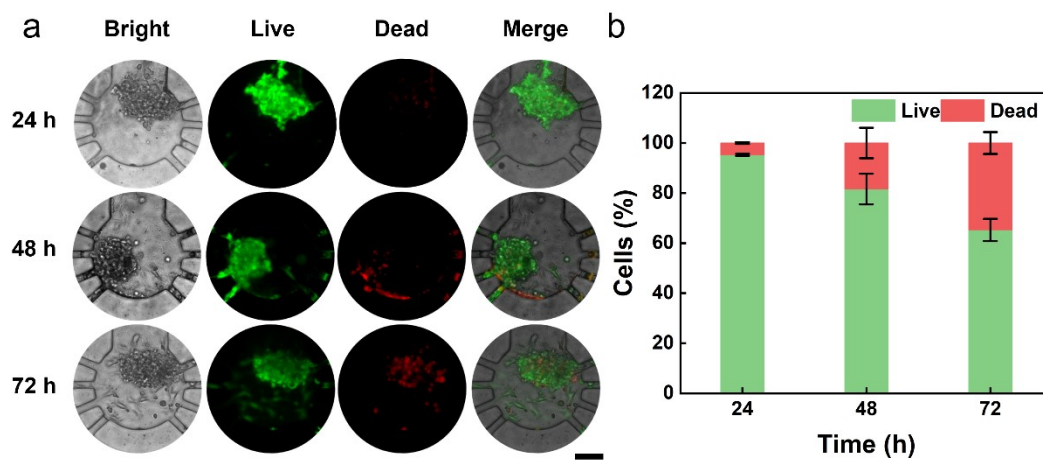


**Fig. S8** Viability assessment of on-Chip tumor spheroids. (a) Microscopic images after 24 h, 48 h, and 72 h culture (green: live cells; red: dead cells. Scale bar: 100  $\mu\text{m}$ ). (b) Histogram of cell viability rates. Error bars represent triplicate experiments.

**Fig. S9 Viability assessment of on-chip HUVECs**

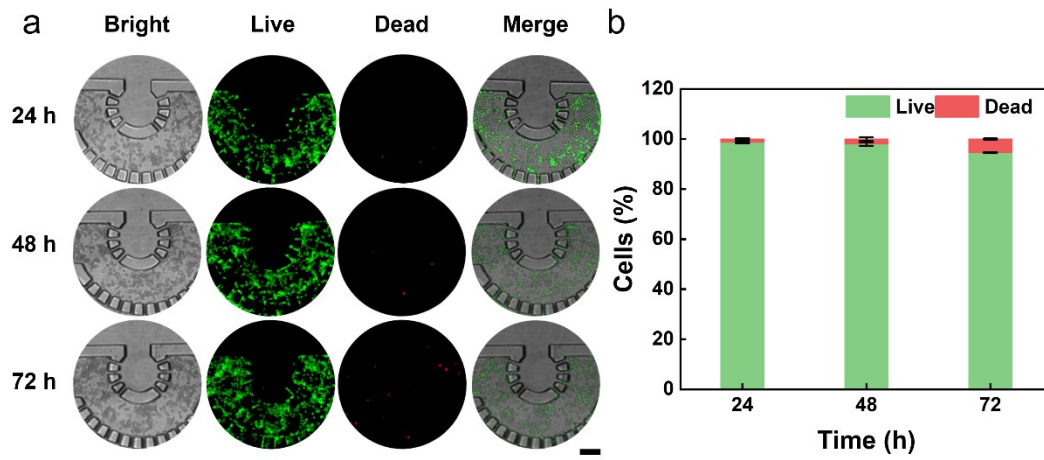


**Fig. S9** Viability assessment of on-chip HUVECs. (a) Microscopic images after 24 h, 48 h, and 72 h culture (green: live cells; red: dead cells. Scale bar: 150  $\mu\text{m}$ ). (b) Histogram of cell viability rates. Error bars represent triplicate experiments.

**Fig. S10** Effects of MDA-MB-231-derived exosomes on tumor invasion and angiogenesis under different incubation times

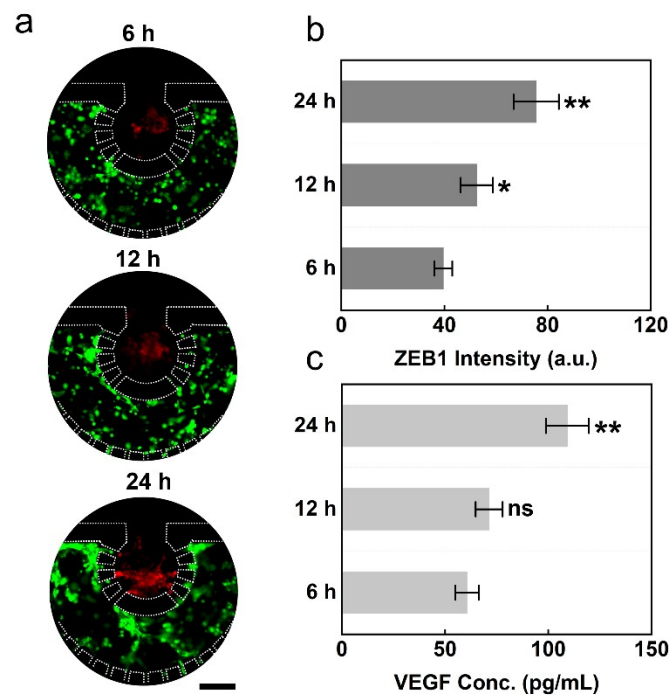


**Fig. S10** Effects of MDA-MB-231-derived exosomes on tumor invasion and angiogenesis under different incubation times. (a) Immunofluorescence images of on-chip co-culture with exosomes ( $10^{12}$  particles/mL with  $10 \mu\text{M}$  gw4869) under different incubation times. Red: ZEB1 (tumor invasion marker), Green: CD31 (vascular endothelial marker). Scale bar:  $150 \mu\text{m}$ . (b) Tumor invasion assessment: Quantitative analysis of ZEB1 fluorescence intensity. Error bars represent standard deviations from triplicate experiments. (c) Angiogenesis evaluation: VEGF concentration measured by ELISA. Error bars indicate standard deviations from triplicate experiments. Statistical significance (two-tailed t-test): In (b) and (c), \* $p$  values compare 12 h and 24 h groups vs. 6 h group: \* $p < 0.05$ , \*\* $p < 0.01$ , \*\*\* $p < 0.001$ , ns = not significant.

**Fig. S11 Construction of Exosome<sup>HSP del</sup>**

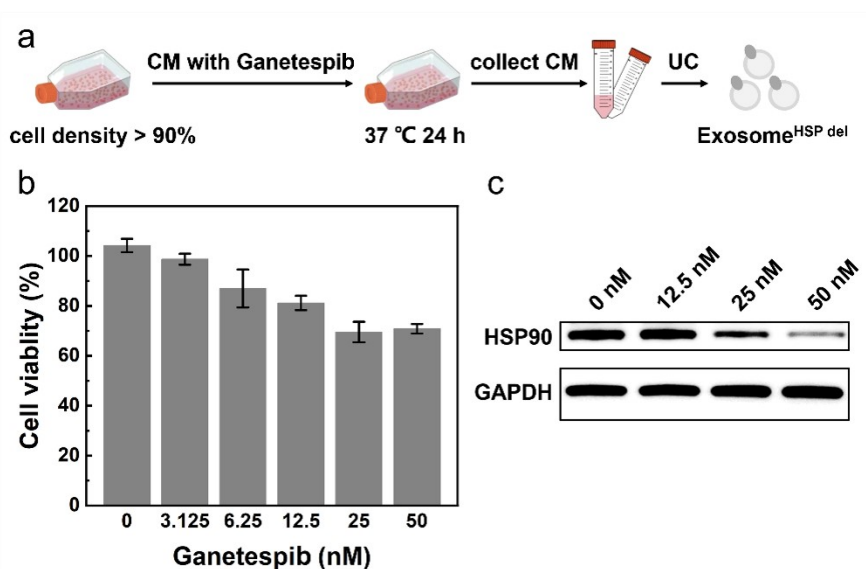


**Fig. S11** Construction of Exosome<sup>HSP del</sup>. (a) Schematic diagram of Exosome<sup>HSP del</sup> construction. CM: Conditioned medium; UC: Ultracentrifugation. (b) Cell viability of MDA-MB-231 cells after 24-hour incubation with different concentrations of GanetespiB at 37 °C. Error bars represent standard deviations from three independent experiments. (c) Western blot analysis of HSP90 protein expression in MDA-MB-231 cells treated with varying concentrations of GanetespiB.

**Fig. S12** The variation trend of Absorbance versus HSP concentration.

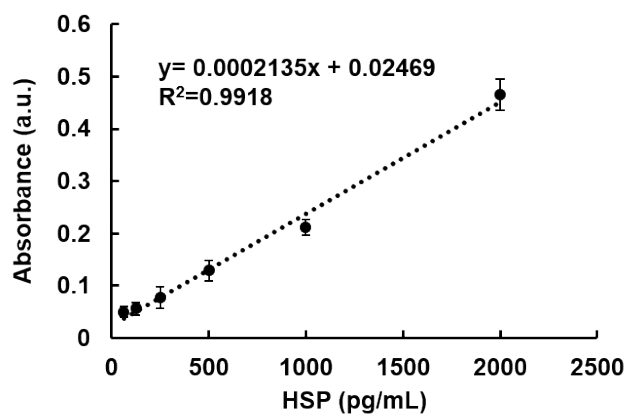


**Fig. S12** The variation trend of Absorbance versus HSP concentration. The linear correlations inset can be described as  $Absorbance = 0.0002135 C_{HSP (pg/mL)} + 0.02469$ . Error bars were derived from three parallel experiments.

**Fig. S13 Effects of HSP90 concentration on tumor invasion and angiogenesis**

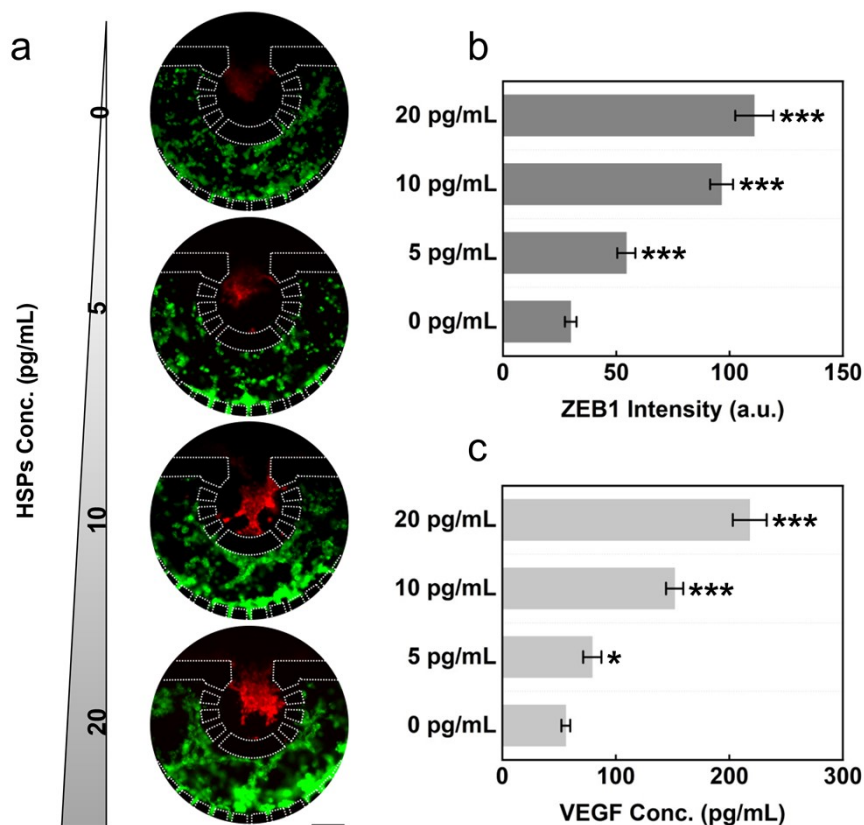


**Fig. S13** Effects of HSP90 concentration on tumor invasion and angiogenesis. (a) Immunofluorescence images after 24-hour on-chip co-culture with different concentrations of HSP90. Red: ZEB1 (tumor invasion marker), Green: CD31 (vascular endothelial marker). Scale bar: 150  $\mu\text{m}$ . (b) Tumor invasion assessment: Quantitative analysis of ZEB1 fluorescence intensity. Error bars represent standard deviations from triplicate experiments. (c) Angiogenesis evaluation: VEGF concentration measured by ELISA. Error bars indicate standard deviations from triplicate experiments. Statistical significance (two-tailed t-test): In (b) and (c), \* $p < 0.05$ , \*\* $p < 0.01$ , \*\*\* $p < 0.001$ , ns = not significant.